

Application of geospatial technologies in developing a dynamic landslide early warning system in a humanitarian context: the Rohingya refugee crisis in Cox's Bazar, Bangladesh

Bayes Ahmed^a , Md. Shahinoor Rahman^{b,c}, Peter Sammonds^a, Rahenul Islam^d and Kabir Uddin^e

^aInstitute for Risk and Disaster Reduction (IRDR), University College London (UCL), London, UK; ^bCentre for Spatial Information Science and Systems, George Mason University, Fairfax, VA, USA; ^cBUET-Japan Institute of Disaster Prevention and Urban Safety (BUET-JIDPUS), Bangladesh University of Engineering and Technology (BUET), Dhaka, Bangladesh; ^dProgramming Division, Planning Commission, Ministry of Planning, Dhaka, Bangladesh; ^eInternational Centre for Integrated Mountain Development (ICIMOD), Kathmandu, Nepal

ABSTRACT

Since August 2017, more than 744,400 stateless Rohingya refugees – an ethnic Muslim minority group from the Rakhine State – have entered Bangladesh to escape serious crimes against humanity conducted by the Myanmar Army. Extensive level of deforestation and hill cutting activities took place in Cox's Bazar District (CBD) in Bangladesh to accommodate them. The refugee camps are sitting on hills and loose soil and are highly vulnerable to rainfall-triggered landslides. Notably in June 2017, landslides in the same region killed at least 160 people. From this perspective, the study aims to develop a localised landslide early warning system (EWS) for the Rohingya refugees and their host communities in CBD. A novel method, combining landslide inventory and susceptibility maps, rainfall thresholds and dynamic web-based alert system, has been introduced to develop the landslide early warning system (EWS) by applying advanced geoinformation techniques. Results suggest that approximately 5,800 hectares of forest land cover disappeared due to the 2017 Rohingya influx. Land cover changes through hill cutting and slope modifications, and unplanned urbanisation are predominantly responsible for slope failures and consecutive 5-day periods of rainfall between 95–220 mm could initiate landslides in high susceptible areas. The EWS would support the local authorities and international organisations in reducing disaster risks and saving lives from landslides in a humanitarian context.

ARTICLE HISTORY

Received 10 November 2019
Accepted 8 February 2020

KEYWORDS

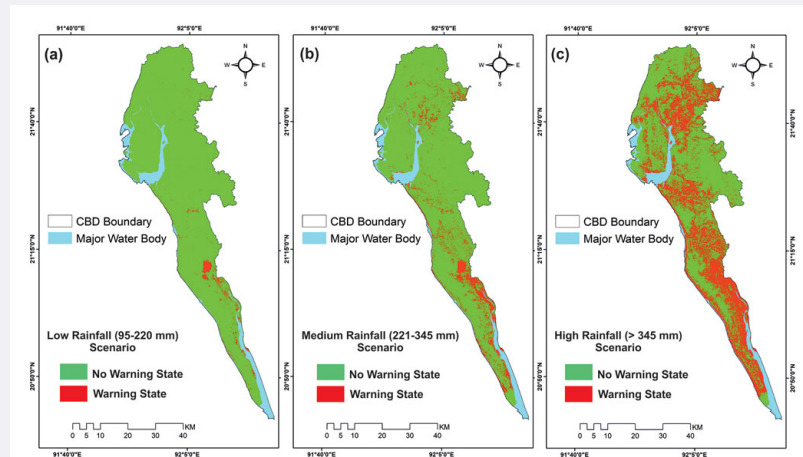
Landslides; GIS; remote sensing; disaster risk reduction; susceptibility mapping; conflict; Rohingya

CONTACT Bayes Ahmed  bayes.ahmed@ucl.ac.uk

 Supplemental data for this article is available online at <https://doi.org/10.1080/19475705.2020.1730988>.

© 2020 The Author(s). Published by Informa UK Limited, trading as Taylor & Francis Group.
This is an Open Access article distributed under the terms of the Creative Commons Attribution License (<http://creativecommons.org/licenses/by/4.0/>), which permits unrestricted use, distribution, and reproduction in any medium, provided the original work is properly cited.

GRAPHICAL ABSTRACT



1. Introduction

Disasters and conflict impact life, livelihood and critical infrastructure. At present, there are around 70.8 million people who were forcibly displaced worldwide and among them 25.9 million are refugees (UNHCR 2018). In most occasions, the refugees are being hosted in developing countries where they live in ecologically degraded environment and areas highly vulnerable to natural hazards (Pollock et al. 2019). To achieve the United Nations (UN) Sustainable Development Goals (SDGs), it is essential to ensure the refugee populations' safety, reduce their disaster vulnerability, and protect the environment.

Landslide disasters are evident in the Chittagong Hill Districts (CHD), located in the southeast region of Bangladesh (Figure 1(a)), that is home to nearly 12 million people (BBS 2014; Ahmed 2017; Rabby and Li 2019). Between 1990 and 2019, a number of catastrophic landslide disasters took over 400 lives and affected 56 thousand people in Bangladesh (Chisty 2014; Rahman et al. 2017). For instance, in June 2017, torrential rainfall-triggered landslides in the CHD claimed at least 162 lives and left 80 thousand inhabitants affected (Ahmed 2017). This study has taken into consideration the Rohingya refugee crisis in Bangladesh as a case study and presented an innovative method by applying advanced geospatial techniques to address issues related to landslide disaster risk reduction (DRR).

Since August 2017, nearly one million Rohingya, an ethnic Muslim minority group from Myanmar, have arrived in Cox's Bazar (Figure 1(b)) to escape an escalation in violence in the Northern Rakhine State. The UN Independent International Fact Finding Mission on Myanmar has quoted this as '*genocide, crimes against humanity and war crimes*', and urges financial isolation of Myanmar military (Human Rights Council 2019). On 23 January 2020, the International Court of Justice (ICJ) has ordered Myanmar to take effective measures to prevent genocide of the Rohingya (ICJ 2019). As of 30 September 2019, the UN High Commissioner for Refugees (UNHCR) has officially registered at least 914,998 Rohingya refugees in the Cox's Bazar District (CBD). This

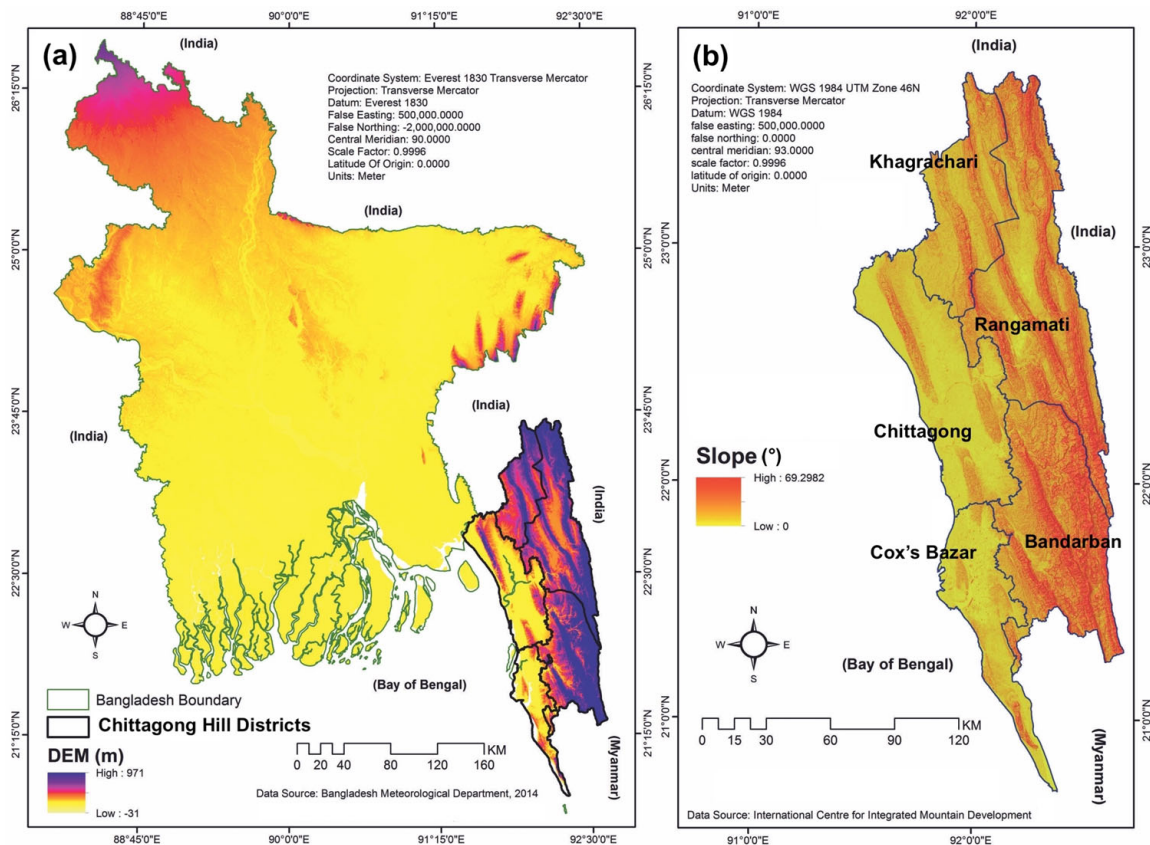


Figure 1. Location of the Chittagong Hill Districts (CHD) in Bangladesh.

number includes 744,400 new arrivals from Myanmar after 25 August 2017 and 33,956 previously registered Rohingya refugees in Bangladesh (UNHCR 2019). In addition, there are still more than 250,000 Rohingyas who are illegally staying outside the official camps as undocumented individuals (Farzana 2017).

The majority of the displaced people are residing in overcrowded temporary make-shift shelters made of bamboo frames, tarpaulin and plastic sheeting in CBD (ISCG 2019). An enormous area of hill forests has already been swiped-out to build the huts by cutting hills and to arrange fuel for cooking. Henceforth, the Rohingya population, mostly women and children, are forced to live in landslide vulnerable camps (Figure 2(a,b)). The 2017 Rohingya exodus has adversely impacted over 336,000 host community members in CBD, who are now in dire need of humanitarian assistance (ISCG 2019). Additionally, the urbanised hilly communities (many of them are also hosting the Rohingyas), predominantly poor and landless people settle in the foothill areas, also live in landslide vulnerable areas (Figure 2(c,d)). It is estimated that around a million people are currently living with landslide risks in CBD; it includes the Rohingya refugees, their host communities, and the urbanized hilly communities (Ahmed 2017; Ahmed, Orcutt, et al. 2018; Ahmed et al. 2020). There is an urgent need to develop and strengthen landslide disaster risk mitigation strategies to support resilient futures for them. In this context, this study aims to develop a landslide early warning system (EWS) for the Rohingya refugees and their host communities in CBD.

Effective early warning systems are instrumental for saving lives, increasing preparedness and reducing the adverse impacts of disasters from natural hazards. The

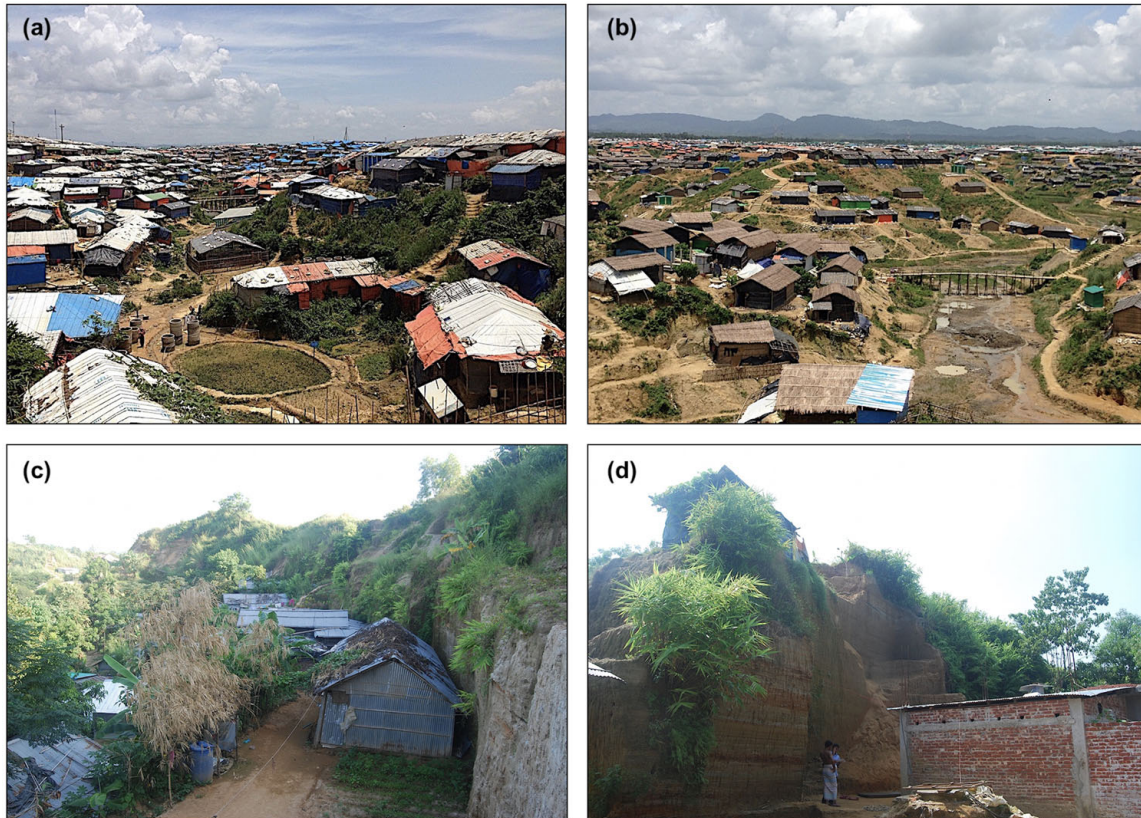


Figure 2. Landslide vulnerable (a, b) Rohingya makeshift camps, and (c, d) urbanised hilly community settlements in Cox's Bazar District (CBD). Source: Fieldwork, 2015–18.

recent advances of satellite based remote sensing (RS), geographic information system (GIS), and earth observation (EO) tools and techniques are contributing significantly in producing landslide hazard maps and EWSs (van Westen et al. 2008; Pisano et al. 2017). Globally a number of frameworks have been proposed to develop EWSs or near-real time situational awareness models for landslide hazard monitoring by combining landslide susceptibility maps (LSM) and rainfall data (Hong and Adler 2007; Kirschbaum and Stanley 2018). For example, Hong et al. (2006) utilized the National Aeronautics and Space Administration's (NASA) tropical rainfall measuring mission (TRMM) data to identify the potential areas of landslides after 1-day, 3-days and 7-days of rainfall at the global-scale. The recent trend of developing regional-scale landslide EWSs is primarily based on combining LSMs (Lagomarsino et al. 2013) and empirical rainfall thresholds (Guzzetti et al. 2007; Gariano et al. 2017; Naidu et al. 2018), and disseminating alerts via Web-GIS based platforms (Segoni et al. 2015, 2018). At the local-scale, the standard practice is to install rain gauges or advanced displacement monitoring systems, analyse area-specific hourly rainfall thresholds, prepare detailed landslide hazard maps, conducting social vulnerability assessment, train community members, and disseminate information (Yin et al. 2010; Karnawati et al. 2011; Intrieri et al. 2012). However, several issues regarding landslide EWSs' design, implementation, communication and management are still in question and need further improvements.

Guzzetti et al. (2019) proposed some recommendations to improve the reliability and credibility of geographical landslide EWSs that include – implementing new and

localised EWSs at high risk areas, addressing local climate and environmental changes, using standard statistical methods for modelling, and appropriately integrating susceptibility maps in operational landslide EWSs. In addition, Peters (2019) suggested to integrate conflict contexts into DRR activities. To overcome the research gaps, this study has emphasised on developing a sub-national scale landslide EWS where the context is intersecting between conflict and disasters (i.e., landslides). The work has also proposed a novel method by dynamically connecting rainfall thresholds and landslide susceptibility zones by applying advanced geoinformation and EO systems in a least developed country (i.e., Bangladesh). The ultimate vision is to advance the current state of knowledge in the fields of DRR and application of geoinformation by focusing on a refugee crisis context.

2. Materials and methods

2.1. The study area: CBD

Cox's Bazar District (CBD) is bounded on the north by Chittagong district (recently renamed as *Chattogram*), on the east by Bandarban district; and on the south-east by Myanmar, the Naf River, and the Bay of Bengal (Figures 1 and 3). The total population of CBD is approximately 2.29 million, excluding the Rohingya refugees, with an area of 2,491.82 km². The annual average rainfall of CBD is 4,288 mm (BBS 2014). The hills of CBD range between 100 to 300 meters. The hill soil is primarily composed of unconsolidated sandstones, siltstones, and shales (Brammer 2012). Climate change also threatens the region with the likelihood of increased precipitation in a short period of time (IPCC 2018). Consequently, CBD and particularly the Rohingya camps are highly prone to cyclones, landslides and flash flooding (Ahmed 2015; Ahmed et al. 2019; Alam et al. 2019). In recent years, CBD has experienced a series of periodic landslide disasters (see [supplementary material](#), Table S1) due to rapid urban growth without proper planning, indiscriminate deforestation and hill cutting. However, the sudden arrival of a million Rohingya refugees in the Ukhia and Teknaf Upazilas (an *Upazila* is a sub-district) has further aggravated landslide risk in the entire district.

The Kutupalong camp (Figure 3(b)) is now considered as the world's most densely populated (with an average density of 75,000 individuals/km²) and largest refugee settlement. Nearly 200,000 refugees are currently living at risk of severe landslides in the camps (UNHCR 2019), whereas, more than three quarters of them are women and children. The host population, who are now outnumbered by the Rohingya refugees, are also struggling to cope with the adverse impacts of deforestation, loss of agricultural lands, health-hazards, groundwater depletion and hill cutting. As for example, since 21 April 2019, monsoon-related events specifically landslides affected more than 50,000 refugees, out of which 6,300 refugees were temporarily displaced, 10 fatalities were reported and 42 refugees were injured (ISCG 2019). The crisis is seen as a threat to the national security of Bangladesh. There are social strains developing between the refugee and host communities. Gross environmental degradation due to the 2017 Rohingya influx has severely increased landslide risks particularly in the Ukhia and Teknaf Upazilas (Figure 3). This has been a matter of great concern

for the government agencies, stakeholders and international communities to protect the devastated forced migrants and affected local host community members in CBD.

2.2. Methodology

This study aims to integrate landslide susceptibility zones, rainfall thresholds, forecasted daily rainfall data, and web-based geospatial technologies to develop a landslide EWS for CBD. Land cover change and hill cutting have been identified as the key triggering factors for landslides in CBD. Land cover maps of four different years (1998, 2001, 2017, and 2018) are considered for change monitoring. The land cover maps are helpful to understand both the general trend of land cover change and the change due to the 2017 Rohingya exodus in Cox's Bazar. The surrounding islands of CBD (e.g., Saint Martin's Island) are excluded from analysis as they are not related to landslides. Landslide susceptibility maps are produced applying multiple regressions (MR) and self-organizing map (SOM) methods. The landslide causative factor maps and updated landslide inventory of the study area have been considered for susceptibility modelling. The landslide susceptibility index map is then categorised into three susceptibility zones – low, medium, and high. Rainfall thresholds for different susceptibility zones are analysed using historical rainfall information following the landslide events. Finally, a web-based landslide early warning system has been developed based on analysing the susceptibility zones, rainfall thresholds, and rainfall forecast. The details of the methodological steps are discussed in the following sub-sections:

2.2.1. Land cover mapping

The land cover maps of four different years were prepared using images from the Landsat satellite missions (Table S2). The images were download from the earth explorer which is an archived data portal of the United States Geological Survey (USGS). An object-based image analysis (OBIA) was applied for the image classification, because of its advantages over other image classification techniques. OBIA tools available in the eCognition software platform was utilized for landcover mapping. OBIA is a combination of both supervised and unsupervised learning of image classification. At first, the image object is assessed through the internal characteristics of data through spatial, spectral, and temporal scale. Images are then segmented based on the spectral response of different landcover types. The multispectral segmentation is used over the Landsat multispectral images to merge thee neighbouring pixels of same land cover types based on relative homogeneity criteria (Hay and Castilla 2008; Bajracharya et al. 2010).

Segments are then grouped together to define image objects by user-defined rules. The image objects are then coded according to their attributes such as normalized difference vegetation index (NDVI), land-water mask, colour, slope, and relative position (Uddin et al. 2015). A harmonized land cover classification system as proposed by Gregorio (2005) was applied. Next, the land cover maps were prepared by labelling a coded group of segments using ground truth information collected from high-resolution Google Earth images. The land cover maps were validated through accuracy assessment. Over one thousand reference pixels were selected through stratified random sampling for the accuracy assessment.

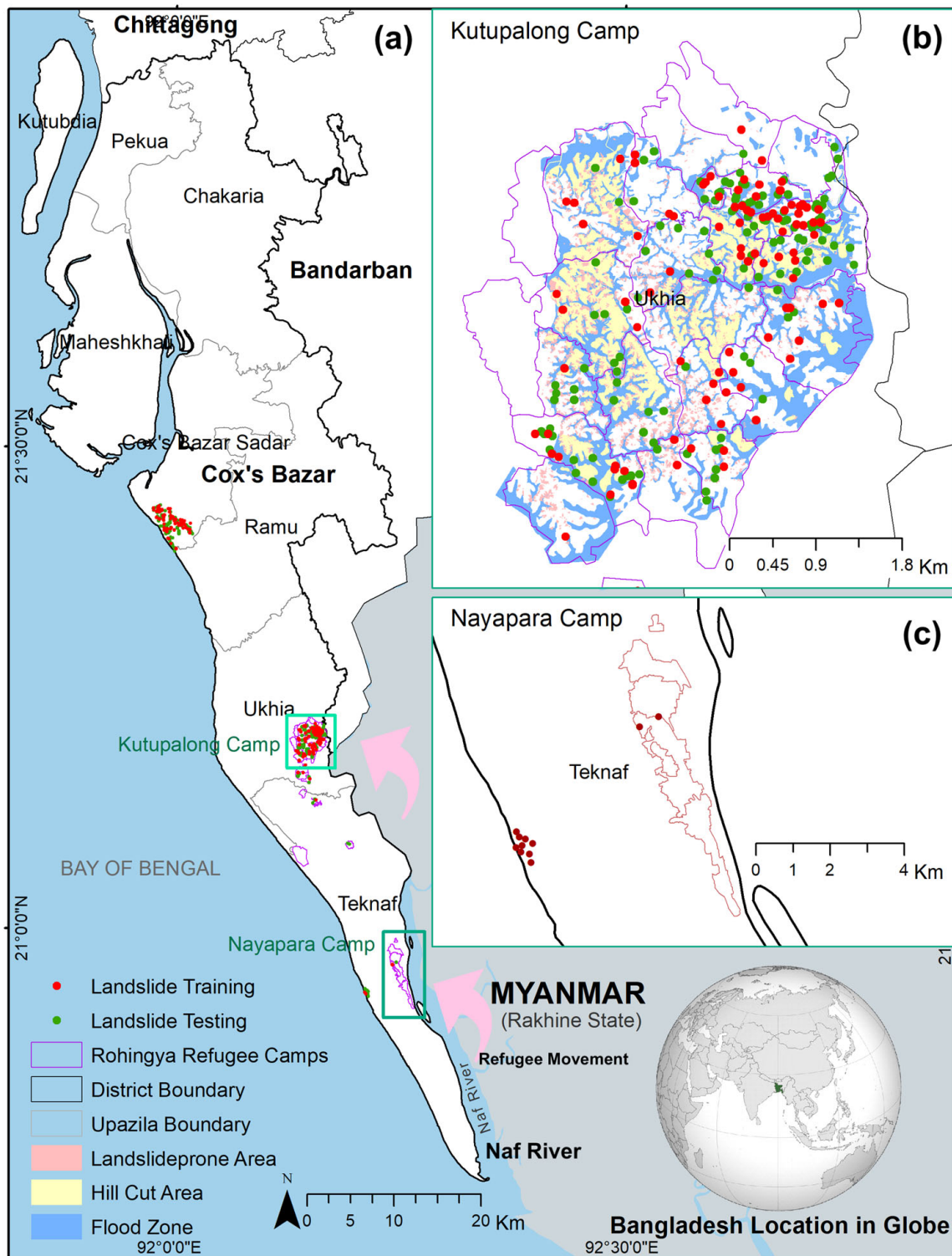


Figure 3. The location of Rohingya refugee camps in Cox's Bazar District (CBD), Bangladesh. Source: Fieldwork and ISCG (2019).

2.2.2. Preparing landslide inventory and factor maps

A detailed and up-to-dated landslide inventory map was prepared through collecting historical landslide information from different organizations and newspapers, and later verifying the locations by reconnaissance and global positioning system (GPS) surveys in the field (Table S1). A landslide investigation form was prepared to collect information on landslide movement type, state, distribution, style, rate, damage,

material, displacement volume, causes of movement and other necessary information (Ahmed 2017). The landslide locations in the Rohingya camps and boundary shape-files were collected from the data portal of the United Nations Office for the Coordination of Humanitarian Affairs (UN-OCHA) (ISCG 2019). Cox's-bazar district and other administrative boundaries were collected from the Cox's Bazar Development Authority (CoxDA). The topography-based landslide causative factors such as slope, aspect, elevation, topographic wetness index (TWI), integrated moisture index (IMI), and stream networks were derived from the digital elevation model (DEM). The Shuttle Radar Topography Mission (SRTM) global ~30-meter spatial resolution DEM (dated: 11 February 2000) was used for this study (LP DAAC 2019). Geological causative factor maps such as surface geology map and fault map were collected from the Geological Survey of Bangladesh. The hill cut map was prepared by analysing landcover change between 1998 and 2018, and respective slope information. Distance to major roads, hill cut, fault, and stream maps were generated using the Euclidian distance from these factors. Finally, all the landslide causative factor maps were projected to the UTM-46N to ensure the same geographic reference.

2.2.3. Landslide susceptibility mapping

Landslide susceptibility is defined as the quantitative or qualitative analysis of classification, area and spatial distribution of landslides that exist or potentially can occur in an area (Couture et al. 2013). LSMs are frequently used for decision making by local authorities. Researchers and experts have produced LSMs using a variety of statistical, weight based, and machine learning methods; notably – the artificial neural network, multiple regressions, weights of evidence, analytic hierarchy process, random forest, and support vector machine algorithms (Gupta et al. 2018; Oh et al., 2018; Valencia Ortiz and Martínez-Graña 2018; Dou et al. 2019; Ahmed et al. 2020).

In this study, MR and SOM methods were applied using the TerrSet software (Eastman 2016). These two methods were successfully applied in previous works to produce scientifically valid LSMs for the Cox's Bazar region (Ahmed 2015). By formulating a linear relationship, the MR determines the probability of being in a particular category of the dependent variable given the independent variables. In this case, the dependent variable was the landslide inventory map which is a dichotomous variable (consists two categories). The landslide factors maps were considered as the independent variables (Eastman 2016). The SOM undertakes a supervised classification of remotely sensed imagery through the artificial neural networks Self-Organizing Map technique (Kohonen 1990; Eastman 2016). Here, the landslide factor maps were considered as input layers where a separate neuron was implied for each reflectance band organised in a two-dimensional array of neurons. A synaptic weight was assigned to all the interconnected input layers to finally produce the output layer or the susceptibility map (Eastman 2016). The two LSMs were validated using the Area Under the relative operating characteristics (ROC) Curve (AUC) method. In determining the statistical reliability of landslide susceptibility maps, an AUC value between 0.7 and 0.9 is scientifically acceptable (Vakhshoori and Zare 2018).

2.2.4. Rainfall threshold analysis

The rainfall thresholds for landslide events were determined through empirical modelling. It is a simple and fewer data demanding method compared to physical models, which require wide-ranging data on various morphological, hydrological, geological, and soil physical properties (Brunetti et al. 2018). The empirical rainfall threshold analysis is mainly a cartesian plotting of rainfall amount of the day of the landslide occurrence versus the amount of antecedent rainfall for few days before the landslide event (Ahmed, Rahman, et al. 2018). Localization of rainfall threshold is one of the most important advantages of the empirical process of rainfall threshold analysis (Calvello et al. 2015). The daily rainfall data between 1960 and 2018 were collected from the Bangladesh Meteorological Department (BMD) and the National Oceanic and Atmospheric Administration (NOAA). The landslide occurrence is highly depended on antecedent rainfall because of the moisture contained in the soil pore. If soil pores already have enough moisture for the slope failure, a landslide can occur even with no or little amount of rainfall. This study has used the information on total rainfall for seven consecutive days prior to a landslide event as the antecedent rainfall. The rainfall threshold was then determined and linked with different landslide susceptibility zones.

2.2.5. Framework for landslide early warning system

The conceptual framework for the development of a landslide early warning system primarily depends on the spatial probability of landslide occurrence (landslide susceptibility) and chances of rainfall above the calculated threshold. The assumption is that the areas with high susceptibility can trigger landslides with low rainfall amount compared to areas with low susceptibility and vice-versa. The conceptual framework of the landslide warning system is explained with the following hypothetical example (see Figure 4). Suppose there is a study area divided into equal sized 36 zones (6×6 grid cells). These zones – No, Low, Medium, High – are classified into four categories based on the landslide susceptibility analysis (Figure 4(a)). Next, after analysing the historical rainfall amount for landslide events in this area, the rainfall rates are categorised into low, medium, and high rainfall events. Landslides can be occurred in high susceptible zones with any rainfall amount. In contrast, there is no chance of occurring landslides in no-susceptible zone whatever the rainfall amounts are. Combining rainfall and landslide susceptibility information, Figure 4(b–d) illustrates the three possible warning scenarios for this hypothetical example. Scenario-1, scenario-2, and scenario-3 shows the possible cells with warning and non-warning states under low, medium, and high rainfall condition, respectively.

2.2.6. Framework for the web-warning system

The warning system was designed based on four major components: susceptibility zonation, rainfall thresholds, forecasted rainfall, and user subscription at the client end. Susceptibility map gives spatial information on possible landslide initiation zones. Rainfall thresholds provide the ranges of rainfall for which landslide may initiate based on the relationship between antecedent and current rainfall. The system collects forecasted rainfall twice a day from an application programming interface (API)

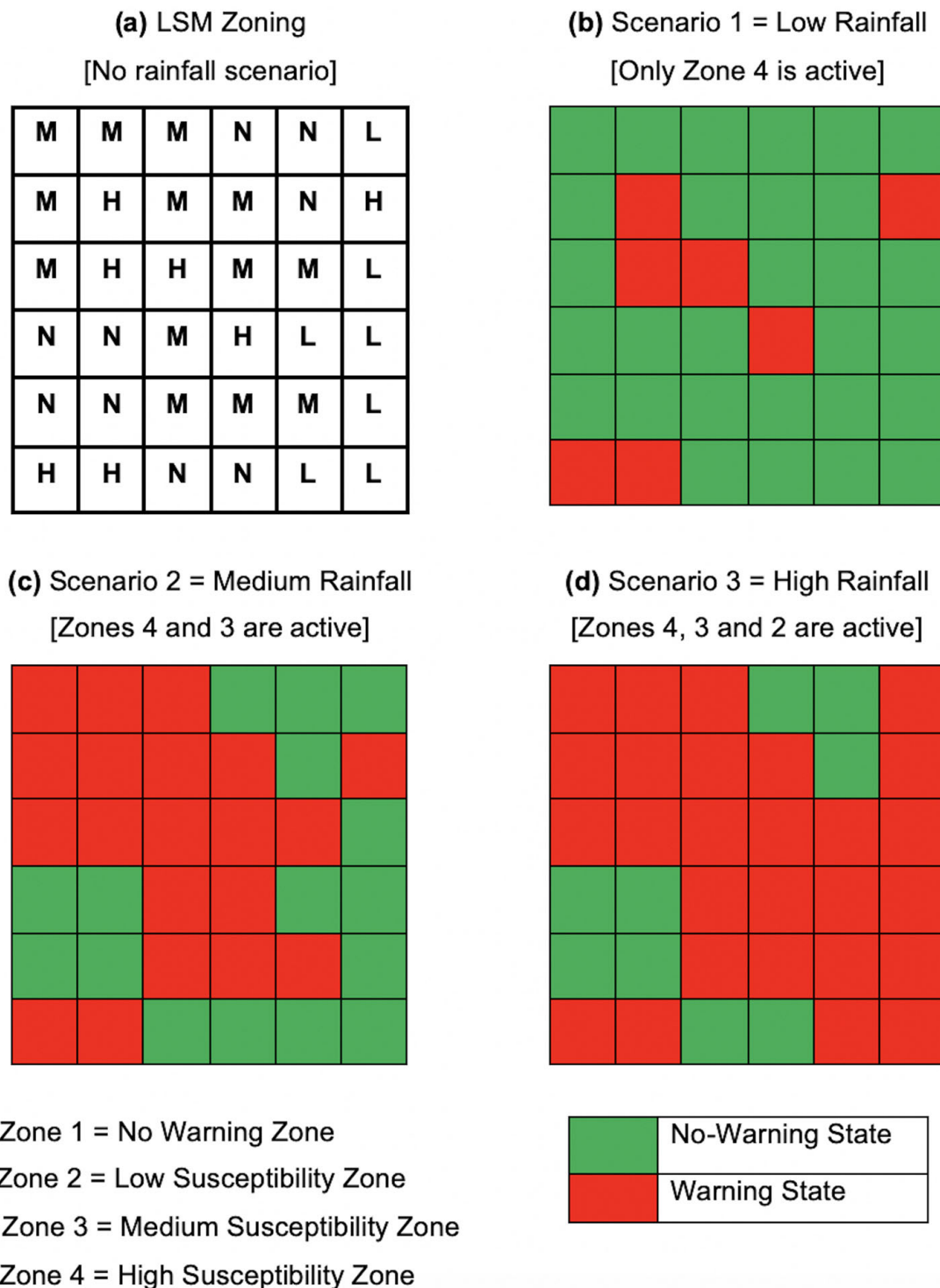


Figure 4. The proposed framework for the landslide early warning system.

operated by the world weather online (www.worldweatheronline.com) for the subsequent five days. The system produces warning zonation maps by incorporating information obtained from the susceptibility zones, rainfall thresholds, and forecasted rainfall. Finally, the warning zonation map is overlaid on the ‘Open Street Map’ for displaying the landslide warning zones in the designated web portal. In addition, the users can subscribe to respective alert zones by registering their email addresses from the landslide warning platform. The system keeps user email addresses in the database to send alerts five days before any possible landslide occurrence.

The warning system has leveraged various frameworks and libraries available from the open source community, such as Python programming language with geospatial data abstraction library (GDAL), MySQL, HTML, PHP, CSS, and JavaScript. The raster LSMs were reclassified using GDAL. MySQL and PHD were utilized for database management at the server end. The system allows the client to interact with warning system through the system user interface. Thus client-side interaction is managed by JavaScript APIs, for instance, the OpenLayers is used for displaying maps in web browsers. Another JavaScript user interface library, W2UI, was deployed for making map layout based on the user query. User queries from client end are managed and send to the server by utilizing jQuery and HTML5.

The susceptibility maps are stored in the system database as a raster database in tiff format for the entire study area. The metadata of raster on the projection system is used for the reprojection of warning zone mapping while overlaying on the open street map. The system creates a special raster format for faster display of alert zones in the rendering process by using PHP. Forecasted precipitation data is stored in a MySQL database. [Figure 5](#) shows the top-level architecture of the landslide early warning system. Static datasets were used to process the landslide susceptibility map and rainfall thresholds. Dynamic data, i.e., forecasted rainfall, is extracted from the external API twice a day. Warning zonation process is run twice a day at the server end to display warning zones at the system interface. A user gets alert only if there is a likelihood of landslides. The methodological steps are illustrated in [Figure 5](#).

3. Results

3.1. Land cover change detection analysis

Seven broad land cover classes, namely – hill forest, shrubland, grassland, cropland, barren land, waterbodies, and builtup areas were chosen ([Figure 6](#)). Please see Table S3 (supplementary document) for more details about the land cover classification. The 1998–2017 land cover changes ([Figure 6\(a,c\)](#)) represent the before Rohingya exodus scenario, and the 2017–2018 ([Figure 6\(c,d\)](#)) changes in land cover represent the after-exodus scenario. The 1998, 2017, and 2018 land cover maps were found to be 78.05%, 91.22%, and 91.44% accurate, respectively (for details see Tables S4–S6 in the supplementary document).

The land cover change analysis indicates that deforestation and urbanisation is prominent in CBD over the years (Table S7 and [Figure S1](#)). Due to the 2017 Rohingya exodus, at least 58 km² forest disappeared ([Figure S1\(d\)](#)). Grassland type that contains deciduous forests was significantly reduced (approx. 235 km²) because of the influx. These two types primarily disappeared for the purpose of constructing new Rohingya makeshift camps and collecting fuel for cooking for the refugee population ([Figure S2](#)). Similar results for land cover changes solely for the Rohingya camps were found by Hassan et al. (2018) and Braun et al. (2019), however, this study covers the entire district.

3.2. Landslide inventory and factor maps

A comprehensive landslide inventory map containing 432 locations for CBD was prepared that was randomly divided into two groups ([Figure 3](#)) – training set for model

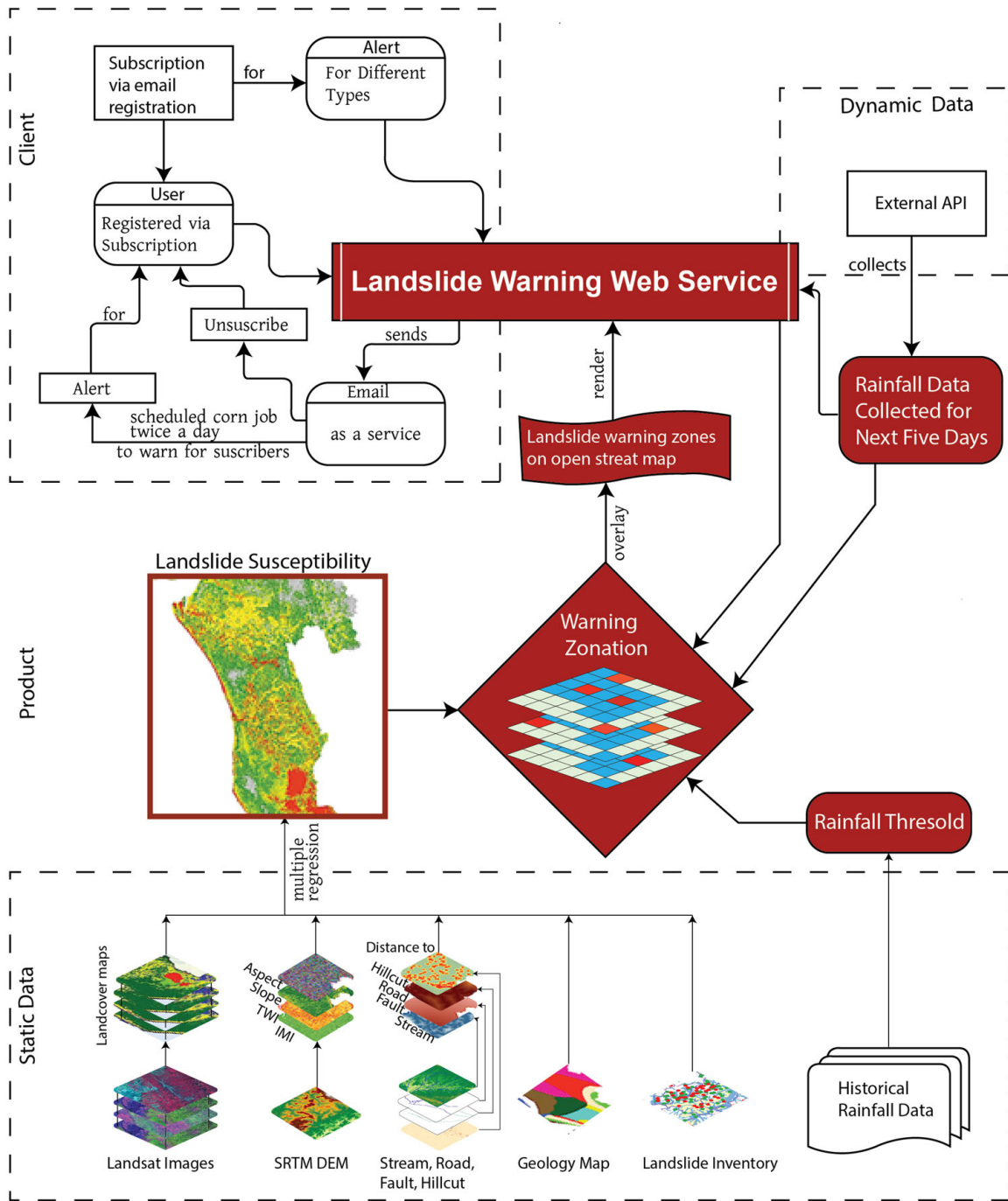


Figure 5. The flowchart of methodology.

running, and testing set for model validation purposes. In CBD, the type of movement was predominantly found as ‘slides’ (rotational and translational), and the engineering soil was categorised as ‘earth slides’. The landslide factor maps are shown in Figure 7. The geology map (Figure 7(b)) was classified as beach and dune sand (csd), Bhuban formation (Miocene, Tb), Boka Bil formation (Neogene, Tbb), Dihing formation (Pleistocene and Pliocene, QTdi), Dihing and Dupi Tila formations undivided (QTdd), Dupi Tila formation (Pleistocene and Pliocene, QTdt), Girujan clay (Pleistocene and Neogene, QTg), Marsh clay and peat (ppc), Tipam Sandstone (Neogene, Tt), valley alluvium and colluvium (ava), and water (H₂O). Boka Bil, Tipam, Dupi Tila, and Dhing formations are actually hilly deposits from the Tertiary

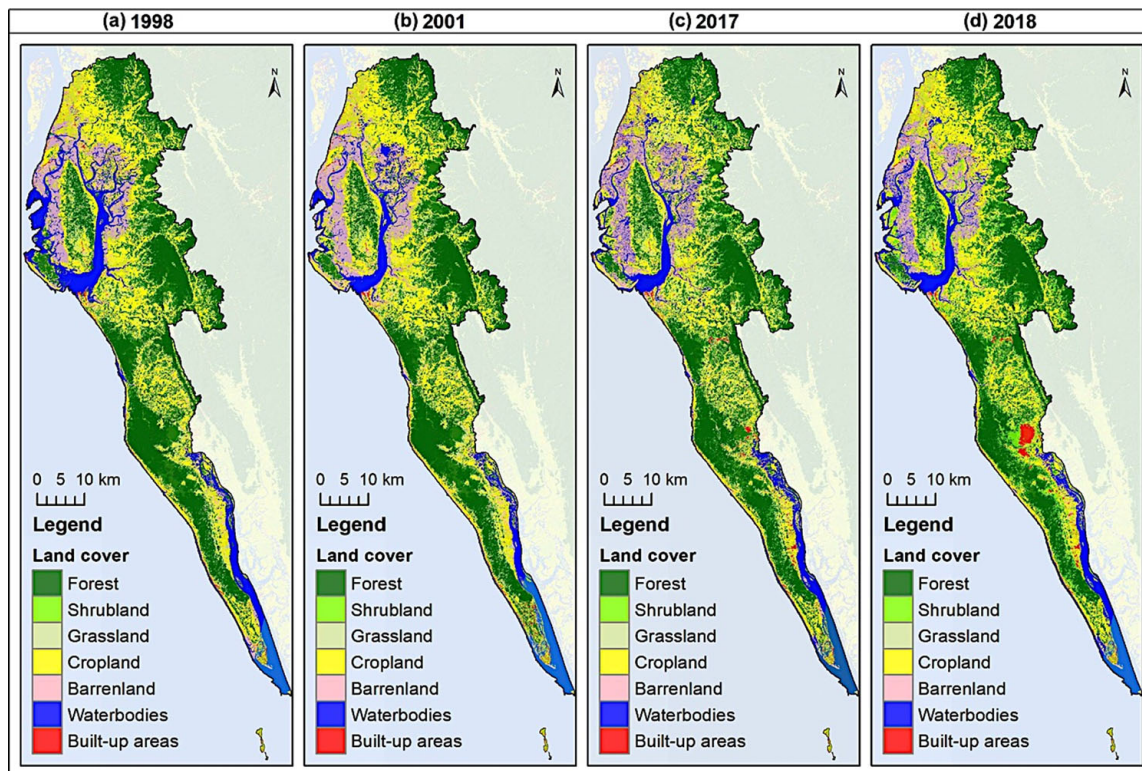


Figure 6. Land cover maps of Cox's Bazar District (CBD).

period. Beach sand and valley formations are from the Quaternary period. Beach sand/tidal deposits are formed near the coast due to tidal actions and are dominated by silt/silt and clay. Valley deposits are formed due to erosional activities near the hilly region and are composed of sand, sandy clay, and silty clay (Brammer 2012).

3.3. Landslide susceptibility modelling results

The landslide training dataset, and the ten factor maps were considered as dependent and independent variables, respectively for producing the MR and SOM LSMs (Figure 8). The ROC AUC values were calculated 0.85 and 0.70 for the MR and SOM, respectively. The MR LSM was selected for further analysis based on higher AUC value.

The 'F-test' and 'T-test' were performed for the overall regression and independent variable's significance analysis, respectively. The statistical hypothesis testing assumes significance at $p < 0.05$. The apparent R ($=0.020568$), apparent R square ($=0.000423$), adjusted R ($=0.020476$) and adjusted R square ($=0.000419$) values were calculated very low. The F-test ($10, 2376995$) $= 100.604408$ result was found significant ($p < 0.0001$). It means the overall MR regression is statistically valid (Table 1). Land cover, slope, and distance from hill-cut variables were found statistically highly significant ($p < 0.0001$) as shown in Table 2. It validates our assumption on strong correlations between landslide occurrences and the relevant independent factor maps (i.e., deforestation, unplanned urbanization, and hill cutting).

Lastly, the MR map was classified into – no warning, and low, medium, and high susceptibility zones as shown in Figure 9(a).

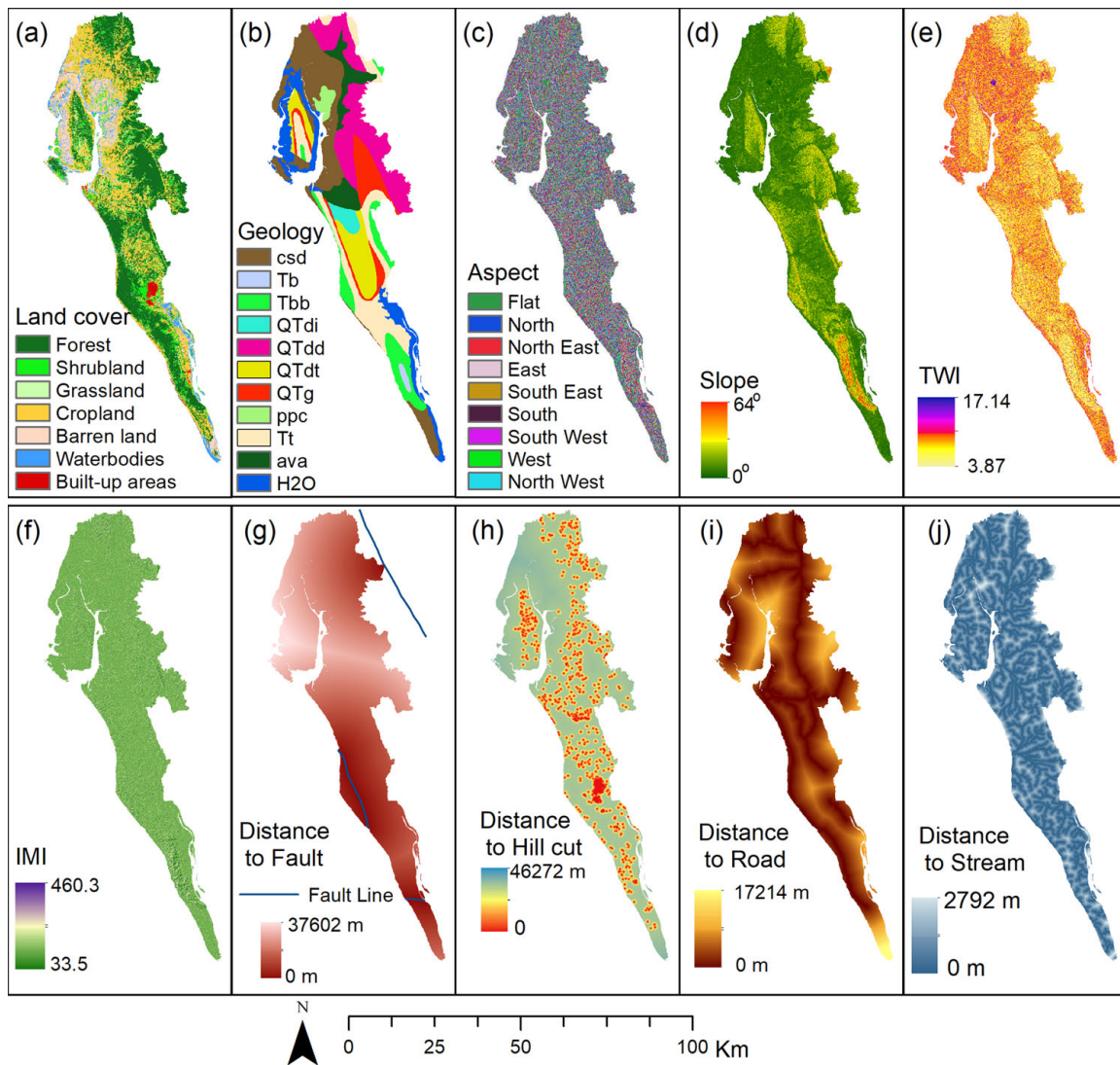


Figure 7. The factor maps used for landslide susceptibility mapping.

3.4. Rainfall threshold analysis results

To calculate the rainfall thresholds, 8-day rainfall data for the major historical landslide events in CBD were analysed. The results reveal that landslides primarily occurred in the months of June and July. As per the median values, 95 mm rainfall in 24 hours, and/or 185 mm rainfall in 48 hours, and/or 241 mm rainfall in 72 hours could trigger landslides in CBD (Table 3). It is also found that landslides are associated with up to 4-day rainfall prior to the events and a landslide warning could be issued accordingly. In this study, 5-day cumulative rainfall ranging between 95–400 mm was considered for rainfall threshold analysis, as around 93% of the median values fitted the model (i.e., coefficient of determinants, $R^2 = 0.93$). Subsequently, the rainfall threshold was classified into three rates: low rainfall (95–220 mm), medium rainfall (221–345 mm), and high rainfall (>345 mm).

In total, 392 landslides were used to validate the proposed method of calculating rainfall thresholds. As per the matrix assumption, the least number of landslides will occur in low rainfall/low susceptibility (R1/S1) zone, and the majority of landslides will occur in high rainfall/high susceptibility zone (R3/S3). The results show that only

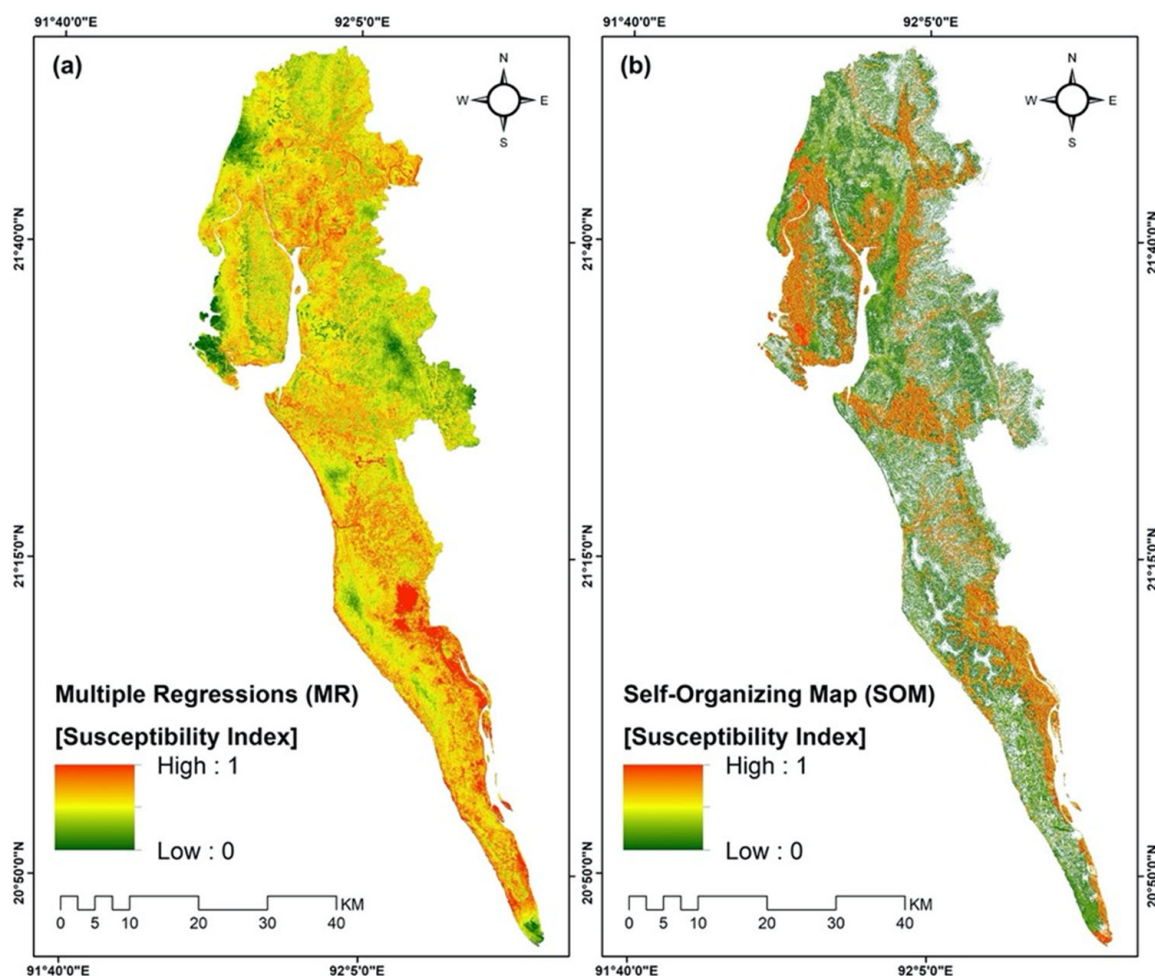


Figure 8. Landslide susceptibility maps of CBD produced by applying the (a) multiple regressions (MR), and (b) self-organizing map (SOM) methods.

one and four landslides were reported in zone R1/S1, and R2/S1, respectively (Table 4). Around 65%, and 63% landslides occurred in high rainfall, and high susceptibility zones, respectively. As assumed, most landslides (132) were observed in zone R3/S3 (Table 4). It proves that the proposed method of combining various rainfall rates and susceptibility classes, as described in this study, is statistically valid.

3.5. Landslide web-warning system development

Table 5 shows the association between landslide susceptibility indices and the (forecasted) rainfall rates. If cumulative rainfall for five consecutive days is forecasted within the limit of low rainfall rate (i.e., 95–220 mm), then the cell values between 0.73–1 would be susceptible to landslides (Table 5). At that point, landslide warnings should be immediately disseminated, and this context has been depicted as ‘Scenario 1’ (Figure 9(b)). Similarly, for the same context, if the total amount of rainfall exceeds 345 mm in 5 days, then areas with cell values between 0.54–1 would receive warnings (Figure 9(d)). LSM cell values between 0–0.53 has been excluded from getting landslide warnings under any circumstances, as it contains low-lands, water bodies, sea beach, and non-hilly areas.

Table 1. ANOVA regression table for the *F*-test.

Model	Apparent degrees of freedom (df)	Sum of squares	Mean square	<i>p</i> -value
Regression	10	0.10	0.01	<0.0001
Residual	2,376,995	246.87	0.00	
Total	2,377,005	246.97		

Table 2. The *T*-test results for the independent variables.

Variable	Coefficient	<i>T</i> -score	<i>p</i> -value
Land cover	0.000118	27.499697	<0.00001
Aspect	−0.000003	−1.041638	0.32239
Fault_dist	−0.000063	−11.870442	<0.00001
Geology	0.000006	2.959666	0.014298
Hill cut_dist	−0.000000	−13.527241	<0.00001
IMI	−0.000011	−1.029410	0.327726
Road_dist	0.000016	2.397961	0.03745
Slope	0.000081	8.738854	<0.00001
Stream_dist	0.000013	2.249783	0.048204
TWI	−0.000018	−2.422774	0.035939

The dynamic web-warning system (WWS) is useful in getting landslide warnings five days in advance and is publicly available at <https://www.landslidebd.com/coxs-bazar-warning/>. The forecasted rainfall values of CBD are updated on a daily basis from the World Weather Online website. The WWS displays 5-day forecasted rainfall values and automatically generates different warning scenarios as described in Table 5 and Figure 9. Anyone can register in the WWS and receive email alerts as per their requirements. The system has a provision to insert rainfall values manually and it also stores previous 30 days rainfall data. It helps the end-users to generate different warning scenarios by utilizing forecasted data collected from other reliable sources.

The EWS effectively predicted the 10 September 2019 landslide event that killed two Bangladeshi (host community) children and injured ten people in the Teknaf area in Cox's Bazar. The event was triggered by 422 mm rainfall in just 24 hours time-frame. At least 15 landslides and 5 flooding incidents were reported in the refugee camps in Teknaf (primarily camp 26) that displaced 14,801 Rohingya refugees, and damaged 427 shelters partially and 66 shelters completely (Figure S3).

4. Discussion

The research paper has four major contributions. First, it has ideally demonstrated the application of advanced geoinformation in land cover and landslide susceptibility mapping, and EWS development. Landslide EWSs are operating in many countries. For example, the U.S. Geological Survey (USGS) issues warnings for rainfall-triggered landslides in the Seattle area solely by analysing rainfall thresholds for landslide activity (USGS 2018), which is a popular trend. However, this study is original as it proposes a method to connect the rainfall thresholds with various landslide hazard zones. The work also addresses some of the recommendations suggested by Guzzetti et al. (2019) regarding geographical landslide EWSs; e.g., developing site-specific EWSs, utilising standard methods for landslide and rainfall threshold models, explaining how susceptibility is used in operational EWSs, and evaluating all parts of a EWS by using user-friendly appropriate tools and criteria.

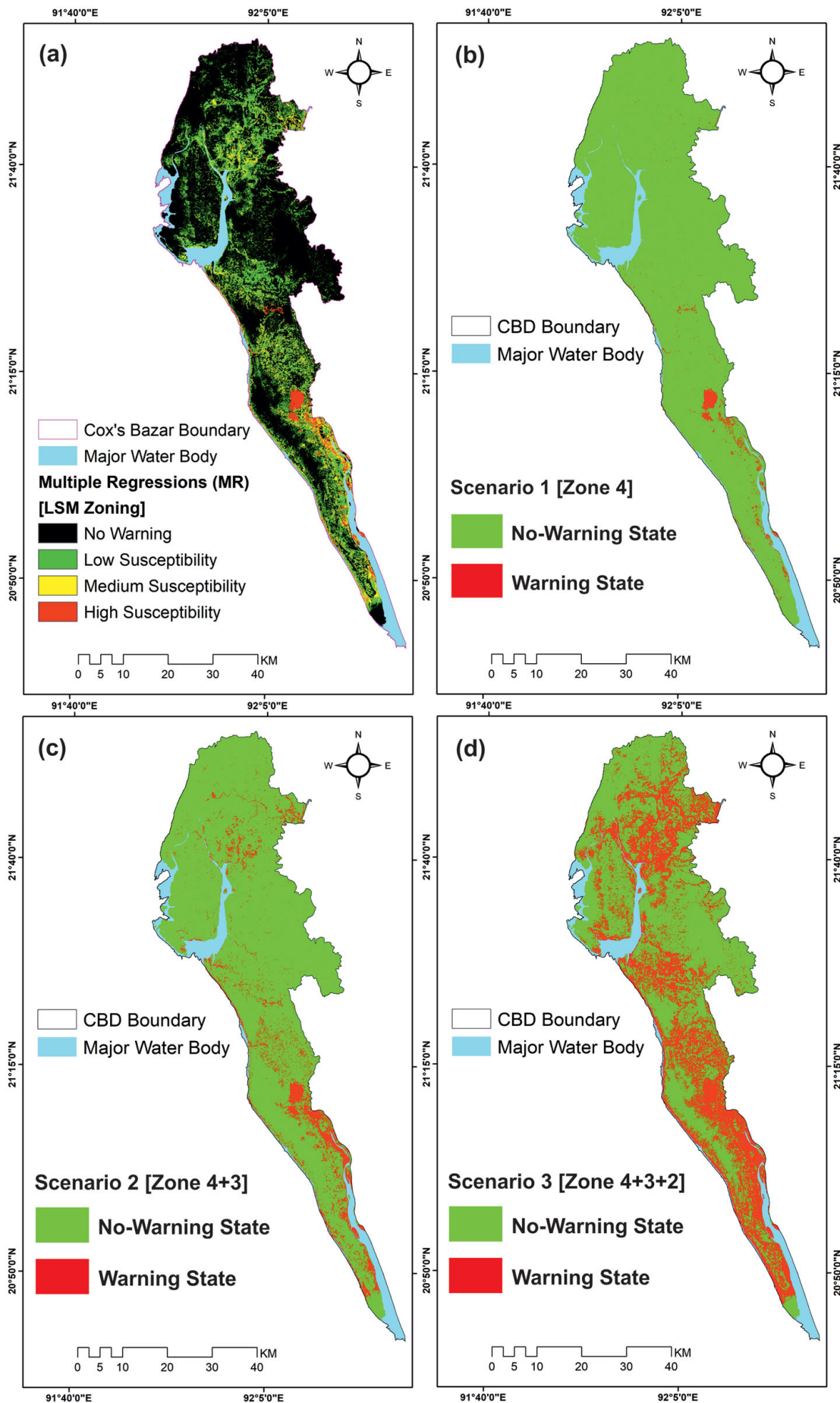


Figure 9. Landslide warning zoning of CBD by applying the multiple regressions method in different scenarios.

Table 3. Relationship between rainfall pattern and triggering landslides in Cox's Bazar District.

ID	Date of the event	Chronology of days							
		-7	-6	-5	-4	-3	-2	-1	0
		Rainfall amount (mm)							
E1	16 June 2003	17	21	110	66	13	42	8	77
E2	29 July 2003	5.08	24.89	0	7.11	36.07	56.90	36.07	82.04
E3	10 June 2006	107.95	11.94	1.02	1.02	41.91	55.12	105.92	117.09
E4	11 June 2007	0.00	0.00	0.00	0.00	36.07	2.03	25.91	181.10
E5	06 July 2007	0.00	16.00	180.59	72.90	58.93	66.04	149.10	21.08
E6	06 July 2008	27	131	188	74	65	100	90	107
E7	29 July 2009	34.04	10.92	28.96	0.00	36.07	51.05	11.94	141.99
E8	15 June 2010	0.00	0.00	0.00	41.91	1.02	74.93	77.98	248.92
E9	26 June 2012	173.99	134.11	0.00	10.92	19.05	32.00	111.00	21.08
E10	27 June 2015	2.03	59.94	74.93	82.04	430.02	255.02	262.89	97.03
E11	27 July 2015	0.00	80.01	41.91	129.03	138.94	213.11	78.99	89.92
E12	04 July 2017	0.00	0.00	5.08	22.10	16.00	71.12	116.08	64.01
E13	25 July 2017	0.00	6.10	103.12	105.92	33.02	167.89	175.01	91.95
E14	10 June 2018	0.00	1.02	0.00	7.87	0.00	0.00	61.98	242.06
E15	12 June 2018	7.87	0.00	0.00	61.98	242.06	66.04	88.90	93.73
E16	25 June 2018	0.00	2.03	0.00	0.00	19.05	42.93	102.11	82.04
E17	04 July 2018	102.11	82.04	4.06	2.03	10.41	29.97	8.89	116.08
E18	25 July 2018	2.29	5.08	3.05	22.61	11.94	35.31	164.34	365.00
Mean		26.63	32.56	41.15	39.30	67.14	75.64	93.06	124.40
Median		02.16	11.43	3.56	22.36	34.55	56.01	89.45	95.38

Here, '6' represents 6 days prior to landslides, and '0' represents the day of the landslide event.

Table 4. Validation results of rainfall rates and landslide susceptibility zones.

Validation matrix	S1 = Zone 2 (low LSM)	S2 = Zone 3 (medium LSM)	S3 = Zone 4 (high LSM)	Total landslides (%)
R1 (low rainfall)	1	11	49	61 (15%)
R2 (medium rainfall)	4	8	66	78 (20%)
R3 (high rainfall)	44	77	132	253 (65%)
Total landslides (%)	49 (13%)	96 (24%)	247 (63%)	392 (100%)

Table 5. Association between landslide susceptibility zoning and rainfall rates.

Rainfall amount (mm) [consecutive 5 days cumulative]	Zone and scenario delineation	LSM index value coverage
Low rainfall (R1) = 95–220	Zone 4 [Scenario 1]	0.73–1
Medium rainfall (R2) = 221–345	Zones 4 + 3 [Scenario 2]	0.62–1
High rainfall (R3) > 345	Zones 4 + 3 + 2 [Scenario 3]	0.54–1
No warning	Zone 1	0–0.53

Second, until today, no landslide EWS is effectively operating in CBD. In 2010, the Government of Bangladesh (GoB) tried to introduce a community-based landslide EWS in some parts of the Cox's Bazar Municipality area, but it failed due to lack of project funding and consequential maintenance (CDMP-II 2012). Currently, landslide warnings are given by the Bangladesh Meteorological Department (BMD), and are solely based on forecast of heavy rainfall at the regional scale. This coarse warning is often recognised as 'ineffective' and 'insufficient' at the local level where the spatial distribution and other geomorphological factors are not considered (Ahmed 2017). Disseminating landslide warnings for a vast area could create panic among the local

residents and they might not rely on the system. The proposed method can resolve this issue and reduce the number of false warnings.

Third, the Inter Sector Coordination Group (ISCG) requested for US\$920.5 million in 2019 to provide the much needed humanitarian assistance for the Rohingya refugees and their host communities in Cox's Bazar. However, as of September 2019, only 37.80% of the appeal is funded (UNHCR 2019). The UN and other non-governmental organisations (NGO) are struggling to meet the basic needs in the camps such as food, shelter, medical care, education, water and sanitation etc. During this difficulty, the proposed landslide EWS – which is simple and easily accessible, developed based on freely available data, and effectively functioning – would be beneficial for the authorities to warn the people at risk well in advance.

Fourth, humanitarian crises triggered by violence and disasters in conflict-affected developing countries can set back hard-won development gains and are barriers to achieving the UN SDGs (Peters 2019). The work particularly addresses two of them. The SDG-15 highlights on sustainable management of forests, half deforestation, restore degraded forest, and increase afforestation. The SDG-11 will cover targets related to sustainable urbanisation, significantly reduce the number of deaths and the number of people affected caused by disasters with a focus on protecting the poor and people in vulnerable situations, and support the least developed countries in line with the Sendai Framework for Disaster Risk Reduction 2015–2030 (UNISDR 2015). The Sendai Framework emphasizes on enhancing disaster preparedness for effective response to build back better. The proposed work directly contributes in tackling these defining challenges as mentioned in the SDGs.

The work has some limitations that could be addressed for future research. First, a detailed (historical) landslide inventory map is missing for CBD. Only information about the major landslide events were collected from various secondary sources and were validated through fieldwork. Second, historical hourly rainfall intensity data is not available from BMD. Recently, BMD and their partners have installed some rain gauges in the region, nevertheless, the data is not public. BMD also does not provide any API services to connect forecasted rainfall data in external websites. Third, hill-cutting is a major concern for Cox's Bazar. The LSM map should be regularly updated by incorporating the most recent land cover, hill cut, road cut, and landslide inventory. The rainfall thresholds should be updated on a regular basis by considering the impacts of regional climate change, cyclone intensities, and consequent rainfall patterns. Fourth, a ~30 meters spatial resolution SRTM DEM (1 arc-second for global coverage) and Landsat images were used for analysis; this is another major drawback. High-resolution DEM and satellite images could be useful for producing better results. Finally, it should be admitted that the effectiveness of a landslide EWS also depends on appropriate community training, planning for evacuation routes and shelters, community vulnerability assessment, and integrating local and indigenous knowledge in emergency planning and disaster management (Ahmed 2017; Guzzetti et al. 2019).

5. Conclusions

Since August 2017, around a million Rohingya refugees fled Myanmar's violent campaign of genocide and ethnic cleansing that is straining Bangladesh. It is considered

as the world's fastest growing refugee crisis in recent times. The stateless Rohingya refugees are now forced to live on temporary hilly camps in CBD that severely restrict permanent and safer constructions. Henceforth, the context emphasizes the importance of preparedness and early warning systems to reduce vulnerability to landslide disasters.

Given the circumstances, a framework for developing a web-based dynamic landslide early warning system has been proposed in this study. The landslide EWS has taken into consideration land cover changes, historical landslide events, local rainfall thresholds, landslide susceptibility maps, and a hazard matrix to dynamically relate 5-day forecasted rainfall and their spatial association with the susceptibility map. The results reveal that an enormous forest area has been wiped out to build the camps in CBD that has significantly increased landslide vulnerability of the Rohingya refugees and their host communities. Landslides in the region largely occur in June and July, and consecutive 5-day cumulative rainfall of 95–220 mm could trigger landslides in high susceptible areas. Based on the hazard matrix combinations, three different warning scenarios (Figure 9) have been proposed.

The study focuses on the complex nexus between conflict and natural (-hazard induced) disasters. The proposed EWS is replicable and can be contextualised in similar settings. The originality and novelty of this work essentially reflects in addressing the Rohingya refugee crisis in Bangladesh with a view to reach the population furthest behind. The work addresses the UN Sustainable Development Goals by promoting the application of geoinformation in natural hazard assessment, environmental planning and disaster risk reduction.

Acknowledgements

We are grateful to the Ministry of Disaster Management and Relief (MoDMR) – Bangladesh, Ministry of Foreign Affairs (MoFA) – Bangladesh, Office of the Refugee Relief and Repatriation Commission (RRRC), University of Dhaka, Cox's Bazar Development Authority, and Health Management BD Foundation for permitting us to enter the Rohingya camps in Cox's Bazar and carry out our research activities. We are also indebted to the Rohingya refugees and members of the host communities for assisting us on numerous occasions.

Disclosure statement

No potential conflict of interest was reported by the authors.

Funding

The study was conducted as part of the project – 'Resilient Futures for the Rohingya Refugees' funded by the Royal Society (Award Reference: CHL\R1\180288).

ORCID

Bayes Ahmed  <http://orcid.org/0000-0001-5092-5528>

References

- Ahmed B. 2015. Landslide susceptibility modelling applying user-defined weighting and data-driven statistical techniques in Cox's Bazar Municipality, Bangladesh. *Nat Hazards*. 79(3): 1707–1737.
- Ahmed B. 2017. Community vulnerability to landslides in Bangladesh [PhD thesis]. London (UK): University College London (UCL).
- Ahmed B, Kelman I, Raja DR, Islam MR, Das S, Shamsudduha M, Fordham M. 2019. Livelihood impacts of flash floods in Cox's Bazar District, Bangladesh. *Int J Mass Emerg Disasters*. 37(3):306–326.
- Ahmed B, Orcutt M, Sammonds P, Burns R, Issa R, Abubakar I, Devakumar D. 2018. Humanitarian disaster for Rohingya refugees: impending natural hazards and worsening public health crises. *Lancet Glob Health*. 6(5):e487–e488.
- Ahmed B, Rahman MS, Islam R, Sammonds P, Zhou C, Uddin K, Al-Hussaini TM. 2018. Developing a dynamic web-GIS based landslide early warning system for the Chittagong metropolitan area, Bangladesh. *IJGI*. 7(12):485.
- Ahmed N, Firoze A, Rahman RM. 2020. Machine learning for predicting landslide risk of Rohingya refugee camp infrastructure. *J Inform Telecommun*. DOI: [10.1080/24751839.2019.1704114](https://doi.org/10.1080/24751839.2019.1704114)
- Alam A, Sammonds P, Ahmed B. 2019. Cyclone risk assessment of the Cox's Bazar District and Rohingya refugee camps in southeast Bangladesh. *Sci Total Environ*. 704:135360.
- Bajracharya B, Uddin K, Chettri N, Shrestha B, Siddiqui SA. 2010. Understanding land cover change using a harmonized classification system in the Himalaya. *Mt Res Dev*. 30(2): 143–156.
- BBS. 2014. Community report, Zila: Cox's Bazar. Bangladesh Population and Housing Census 2011. Bangladesh Bureau of Statistics (BBS), Statistics and Informatics Division (SID), Ministry of Planning, Dhaka, Government of the People's Republic of Bangladesh.
- Brammer H. 2012. The physical geography of Bangladesh. Dhaka (Bangladesh): The University Press Limited.
- Braun A, Fakhri F, Hochschild V. 2019. Refugee camp monitoring and environmental change assessment of Kutupalong, Bangladesh, based on radar imagery of sentinel-1 and ALOS-2. *Remote Sens*. 11(17):2047.
- Brunetti MT, Melillo M, Peruccacci S, Ciabatta L, Brocca L. 2018. How far are we from the use of satellite rainfall products in landslide forecasting? *Remote Sens Environ*. 210:65–75.
- Calvello M, d'Orsi RN, Piciullo L, Paes N, Magalhaes M, Lacerda WA. 2015. The Rio de Janeiro early warning system for rainfall-induced landslides: analysis of performance for the years 2010–2013. *Int J Disaster Risk Reduct*. 12:3–15.
- CDMP-II. 2012. Landslide inventory and land-use mapping, DEM Preparation, Precipitation Threshold Value and Establishment of Early Warning Devices. Comprehensive Disaster Management Programme-II (CDMP-II), Ministry of Food and Disaster Management, Disaster Management and Relief Division, Government of the People's Republic of Bangladesh.
- Chisty KU. 2014. Landslide in Chittagong City: a perspective on hill cutting. *J Bangladesh Inst Plan*. 7:1–17.
- Couture R, Blais-Stevens A, Bobrowsky P, Wang B, VanDine D. 2013. Canadian technical guidelines and best practices related to landslides: a national initiative for loss reduction. In: Sassa K (Ed.), *Landslides: global risk preparedness*. Berlin (Germany): Springer, p. 315–322.
- Dou J, Yunus AP, Tien Bui D, Merghadi A, Sahana M, Zhu Z, Chen C-W, Khosravi K, Yang Y, Pham BT. 2019. Assessment of advanced random forest and decision tree algorithms for modeling rainfall-induced landslide susceptibility in the Izu-Oshima Volcanic Island, Japan. *Sci Total Environ*. 662:332–346.
- Eastman JR. 2016. *TerrSet-geospatial monitoring and modeling system: manual*. Worcester (MA): Clark Labs, Clark University.

- Farzana KF. 2017. *Memories of Burmese Rohingya refugees: contested identity and belonging*. New York (NY): Palgrave Macmillan.
- Gariano SL, Rianna G, Petrucci O, Guzzetti F. 2017. Assessing future changes in the occurrence of rainfall-induced landslides at a regional scale. *Sci Total Environ*. 596:417–426.
- Gregorio AD. 2005. *Land cover classification system classification concepts and user manual Software version (2)*. Rome (Italy): Food and Agriculture Organization of the United Nations.
- Gupta SK, Shukla DP, Thakur M. 2018. Selection of weightages for causative factors used in preparation of landslide susceptibility zonation (LSZ). *Geomatics Nat Hazards Risk*. 9(1): 471–487.
- Guzzetti F, Gariano SL, Peruccacci S, Brunetti MT, Marchesini I, Rossi M, Melillo M. 2019. Geographical landslide early warning systems. *Earth Sci Rev*. 200:102973.
- Guzzetti F, Peruccacci S, Rossi M, Stark CP. 2007. Rainfall thresholds for the initiation of landslides in central and southern Europe. *Meteorol Atmos Phys*. 98(3–4):239–267.
- Hassan M, Smith A, Walker K, Rahman M, Southworth J. 2018. Rohingya refugee crisis and forest cover change in Teknaf, Bangladesh. *Remote Sens*. 10(5):689.
- Hay GJ, Castilla G. 2008. Geographic object-based image analysis (GEOBIA): a new name for a new discipline. In: Blaschke T, Lang S, Hay G, editors. *Object-based image analysis*. New York (NY): Springer, p. 75–90.
- Hong Y, Adler R, Huffman G. 2006. Evaluation of the potential of NASA multi-satellite precipitation analysis in global landslide hazard assessment. *Geophys Res Lett*. 33, L22402, 1–5.
- Hong Y, Adler RF. 2007. Towards an early-warning system for global landslides triggered by rainfall and earthquake. *Int J Remote Sens*. 28(16):3713–3719.
- Human Rights Council. 2019. *Independent International Fact-Finding Mission on Myanmar*. The Office of the High Commissioner for Human Rights (OHCHA). [accessed on 2019 Sept 4]. <https://www.ohchr.org/en/hrbodies/hrc/myanmarffm/pages/index.aspx>.
- ICJ. 2019. *Application of the Convention on the Prevention and Punishment of the Crime of Genocide (The Gambia v. Myanmar)*. International Court of Justice (ICJ), the Hague, Netherlands. [accessed on 2020 Feb 19]. <https://www.icj-cij.org/en/case/178>.
- Intrieri E, Gigli G, Mugnai F, Fanti R, Casagli N. 2012. Design and implementation of a landslide early warning system. *Eng Geol*. 147:124–136.
- IPCC. 2018. *Global warming of 1.5 °C*. The Intergovernmental Panel on Climate Change (IPCC). [accessed on 2019 Feb 21]. <http://www.ipcc.ch/report/sr15/>.
- ISCG. 2019. *Inter Sector Coordination Group (ISCG)*. United Nations Office for the Coordination of Humanitarian Affairs (OCHA). [accessed on 2019 Aug 31]. <https://data.humdata.org/event/rohingya-displacement>.
- Karnawati D, Fathani TF, Ignatius S, Andayani B, Legono D, Burton PW. 2011. Landslide hazard and community-based risk reduction effort in Karanganyar and the surrounding area, central Java, Indonesia. *J Mt Sci*. 8(2):149–153.
- Kirschbaum D, Stanley T. 2018. Satellite-based assessment of rainfall-triggered landslide hazard for situational awareness. *Earths Future*. 6(3):505–523.
- Kohonen T. 1990. The self-organizing map. *Proc IEEE*. 78(9):1464–1480.
- Lagomarsino D, Segoni S, Fanti R, Catani F. 2013. Updating and tuning a regional-scale landslide early warning system. *Landslides*. 10(1):91–97.
- LP DAAC. 2019. *LP DAAC ARCHIVER*. The Land Processes Distributed Active Archive Center (LP DAAC). U.S. Geological Survey, Earth Resources Observation and Science (EROS), Center Sioux Falls, South Dakota 57198, USA. [accessed on 2019 Dec 23].
- Naidu S, Sajinkumar KS, Oommen T, Anuja VJ, Samuel RA, Muraleedharan C. 2018. Early warning system for shallow landslides using rainfall threshold and slope stability analysis. *Geosci Front*. 9(6):1871–1882.
- Oh HJ, Kadavi PR, Lee CW, Lee S. 2018. Evaluation of landslide susceptibility mapping by evidential belief function, logistic regression and support vector machine models. *Geomatics Nat Hazards Risk*. 9(1):1053–1070.

- Peters K. 2019. Disaster risk reduction in conflict contexts: an agenda for action. London (UK): Overseas Development Institute (ODI).
- Pisano L, Zumpano V, Malek Ž, Roskopf CM, Parise M. 2017. Variations in the susceptibility to landslides, as a consequence of land cover changes: a look to the past, and another towards the future. *Sci Total Environ.* 601:1147–1159.
- Pollock W, Wartman J, Abou-Jaoude G, Grant A. 2019. Risk at the margins: a natural hazards perspective on the Syrian refugee crisis in Lebanon. *Int J Disaster Risk Reduct.* 36:101037.
- Rabby YW, Li Y. 2019. An integrated approach to map landslides in Chittagong Hilly Areas, Bangladesh, using Google Earth and field mapping. *Landslides.* 16(3):633–645.
- Rahman MS, Ahmed B, Di L. 2017. Landslide initiation and runout susceptibility modeling in the context of hill cutting and rapid urbanization: a combined approach of weights of evidence and spatial multi-criteria. *J Mt Sci.* 14(10):1919–1937.
- Segoni S, Battistini A, Rossi G, Rosi A, Lagomarsino D, Catani F, Moretti S, Casagli N. 2015. An operational landslide early warning system at regional scale based on space–time-variable rainfall thresholds. *Nat Hazards Earth Syst Sci.* 15(4):853–861.
- Segoni S, Tofani V, Rosi A, Catani F, Casagli N. 2018. Combination of rainfall thresholds and susceptibility maps for dynamic landslide hazard assessment at regional scale. *Front Earth Sci.* 6:85.
- Uddin K, Shrestha HL, Murthy M, Bajracharya B, Shrestha B, Gilani H, Pradhan S, Dangol B. 2015. Development of 2010 national land cover database for the Nepal. *J Environ Manage.* 148:82–90.
- UNHCR. 2018. Global Trend – Forced Displacement in 2017. United Nations High Commissioner for Refugees (UNHCR), Geneva, Switzerland. [accessed on 2019 Sept 4]. <https://www.unhcr.org/uk/figures-at-a-glance.html>.
- UNHCR. 2019. Refugee response in Bangladesh: operational portal. The United Nations High Commissioner for Refugees (UNHCR). [accessed on 2019 Aug 30]. https://data2.unhcr.org/en/situations/myanmar_refugees.
- UNISDR. 2015. Sendai Framework for Disaster Risk Reduction 2015–2030. The United Nations Office for Disaster Risk Reduction (UNISDR). [accessed on 2019 Aug 8]. <https://www.unisdr.org/we/inform/publications/43291>.
- USGS. 2018. Landslide Hazards. The U.S. Geological Survey (USGS). [accessed on 2019 Mar 26]. <https://www.usgs.gov/natural-hazards/landslide-hazards>.
- Vakhshoori V, Zare M. 2018. Is the ROC curve a reliable tool to compare the validity of landslide susceptibility maps? *Geomatics Nat Hazards Risk.* 9(1):249–266.
- Valencia Ortiz JA, Martínez-Graña AM. 2018. A neural network model applied to landslide susceptibility analysis (Capitanejo, Colombia). *Geomatics Nat Hazards Risk.* 9(1):1106–1128.
- van Westen CJ, Castellanos E, Kuriakose SL. 2008. Spatial data for landslide susceptibility, hazard, and vulnerability assessment: an overview. *Eng Geol.* 102(3–4):112–131.
- Yin Y, Wang H, Gao Y, Li X. 2010. Real-time monitoring and early warning of landslides at relocated Wushan Town, the Three Gorges Reservoir, China. *Landslides.* 7(3):339–349.

1

Supplementary Material

2

Table S1. Major landslide disasters in the Cox’s Bazar District, Bangladesh.

Date	Location of Landslides	Rainfall Sequence	Consequences
16 June 2003	Light House Para, Cox’s Bazar	474 mm – 12 days 4 – 15 June 2003	6 fatalities and 2 injuries
29 July 2003	Kalatali, Cox’s Bazar	330 mm – 11 days 19 – 28 July 2003	6 killed and 9 injuries
3 July 2008	Cox’s Bazar Sadar/ Municipality (CBM)	688 mm – 7 days 26 June – 2 July	12 fatalities and several injured
6 July 2008	Teknaf, Cox’s Bazar	981 mm – 10 days 26 June – 5 July	4 people killed
7 April 2010	Ramu, Cox’s Bazar District	No rainfall, but landslide occurred	2 fatalities and several injuries
15 June 2010	Different locations in Bandarban and Cox’s Bazar districts	523 mm – 6 days 10 – 15 June 2010	47 fatalities in Cox’s Bazar and 7 in Bandarban and over 100 injured
26 June 2015	Ramu, Saint Martin; Ghonapara, Lighthouse Para and Shahittika Polli in Cox’s Bazar Municipality	978 mm – 4 days 23 – 26 June 2015	8 killed, 100 villages flooded, 1000 houses damaged, roads damaged, 2 people untraced and many injured
28 June 2015	Teknaf, Ramu, Chokoria, and Pekua Upazila, Cox’s Bazar	5 days of heavy rainfall (674 mm)	21 killed, roads and municipalities are flooded
27 July 2015	South Baharchharha area, Cox’s Bazar	682 mm rainfall in 6 days	5 fatalities, and 4 houses buried
13 June 2017	All five hill districts	300 mm rainfall in 24 hours	159 killed and 88 injured
25 July 2017	Sadar and Ramu Upazila, Cox’s Bazar	677 mm rainfall in 6 days	5 killed and 5 injured
11 June 2018	Ukhia Rohingya camps	459 mm rainfall in 4 days	1 killed and 500 injured

Date	Location of Landslides	Rainfall Sequence	Consequences
12 June 2018	Maheshkhali Upazila		1 killed
25 July 2018	Miar Ghona, CBM and Dokkhin Mithachori, Ramu Upazila	228 mm rainfall in 24 hours	5 killed
May–July 2019	Ukhia Rohingya Camps, Cox’s Bazar	Several days of continuous rainfall	Landslides affected more than 50,000 refugees, 6,300 refugees were temporarily displaced, 10 fatalities have been reported and 42 refugees have been injured
10 September 2019	Notun Pollan Para, Teknaf, Cox’s Bazar	422 mm rainfall in 24 hours	2 children killed and 6 injured

Source: Ahmed, 2017 and national daily newspapers.

3
4
5
6

Table S2. Details of the satellite images used for land cover mapping.

Serial No	Satellite/Sensor	Row No	Path No	Date (dd/mm/yyyy)	Cloud Cover (%)
1	Landsat TM	136	45	27/03/1998	0.00
2	Landsat TM	136	45	31/10/2001	0.00
3	Landsat 8	136	45	15/03/2017	0.05
4	Landsat 8	136	45	02/03/2018	0.02

7
8

Table S3. Land cover classification system.

Land cover classification	Label
A3 = Trees (Main Layer) A11 = Open General (60-70%) – (20- 10%) (Main Layer) B2 = >30- 3 m (Tree height Main Layer) D1 = Broadleaved E1 = Evergreen E4 = Semi-Deciduous or Semi-Evergreen Zt38 = Floristic Aspect: Artocarpus chaplasha, Dipterocarpus spp	Forest
A4 = Shrubs (Main Layer) A10 = Close > 60-70% Main Layer B3 = 5-0.3m (Shrubs Height Main Layer) D1 = Broadleaved E1 = Evergreen L2 = Sloping Land L8 = Hilly Terrain	Shrubland
A6 = Graminoids A10 = Deciduous B4 = 3 - 0.03 m (Herbaceous Height Main Layer) A5 = Bare Soil and/or Other Unconsolidated Material(s)	Grassland
A3 = Herbaceous Crops C3 = One Additional Crop B2= Small Sized Field(s)	Cropland
A2 = Unconsolidated Bare Area	Barren land

Land cover classification	Label
A5 = Bare Soil & Unconsolidated Material	
A1= Inland Water	Waterbodies
A4 = Built Up Area – Non-Linear A13 = Urban Area(s) A15 = Medium Density	Builtup areas

Source: Gregorio, 2005.

10

11

12

Table S4. Land cover classification accuracy of 2018.

Land cover	Forest	Shrubland	Grassland	Cropland	Barren land	Waterbodies	Built-up areas	Total	User's Accuracy (%)
Forest	359	16		8				383	93.73
Shrubland	10	88	2	3			2	105	83.81
Grassland		1	38	2	2	2		45	84.44
Cropland	14		2	272	1	1		290	93.79
Barren land			1	3	74	6		84	88.10
Waterbodies			1	1	7	88		97	90.72
Built-up areas			1	1			10	12	83.33
Total	383	105	45	290	84	97	12		
Producer's Accuracy (%)	93.73	83.81	84.44	93.79	88.10	90.72	83.33		

13

Total Number of Samples	1016	Standard Error of kappa	0.02
No. of Accurate Samples	929	95% Confidence Interval	0.770 to 0.850
Overall Accuracy (%)	91.44	Weighted Kappa	0.906
Kappa	0.81		

14

15

Table S5. Land cover classification accuracy of 2017.

Land Cover	Forest	Shrubland	Grassland	Cropland	Barren land	Waterbodies	Built-up areas	Total	User's Accuracy (%)
Forest	359	16		6				381	94.23
Shrubland	10	88	2	3			2	105	83.81
Grassland		1	37	2	3	2		45	82.22
Cropland	14		1	272	2	1		290	93.79
Barren land			1	4	72	7		84	85.71
Waterbodies			1	2	7	87		97	89.69
Built-up areas			1	1			10	12	83.33
Total	383	105	43	290	84	97	12		
Producer's Accuracy (%)	93.73	83.81	86.05	93.79	85.71	89.69	83.33		

16

Total Number of Samples	1014	Standard Error of kappa	0.02
No. of Accurate Samples	925	95% Confidence Interval	0.770 to 0.850
Overall Accuracy (%)	91.22	Weighted Kappa	0.906
Kappa	0.81		

17

18

19

20

21

22

23

24

Table S6. Land cover classification accuracy of 1998.

25

Land Cover	Forest	Shrubland	Grassland	Cropland	Barren land	Waterbodies	Built-up areas	Total	User's Accuracy (%)
Forest	368	46	6	13	7	3	5	448	82.14
Shrubland	0		0					0	
Grassland	6	41	35	7	1	1	3	94	37.23
Cropland	9	4	1	255	2	5	3	279	91.40
Barren land		8	3	5	62	16		94	65.96
Waterbodies		6		10	12	72		100	72.00
Built-up areas							1	1	100.00
Total	383	105	45	290	84	97	12		
Producer's Accuracy (%)	96.08	0.00	77.78	87.93	73.81	74.23	8.33		

26

Total Number of Samples	1016	Standard Error of kappa	0.02
No. of Accurate Samples	793	95% Confidence Interval	0.770 to 0.850
Overall Accuracy (%)	78.05	Weighted Kappa	0.906
Kappa	0.81		

27

28

29

30

31

32

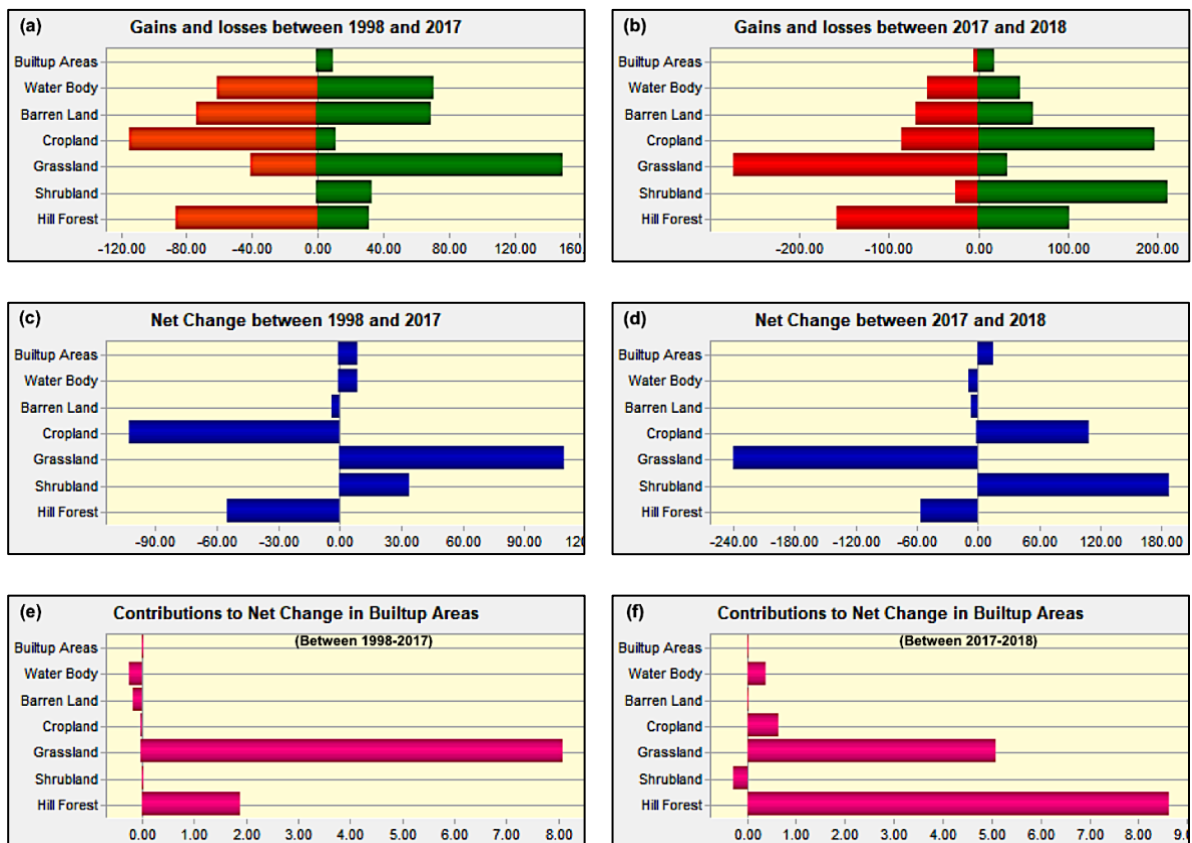
33

34

Table S7. Land cover change pattern in CBD.

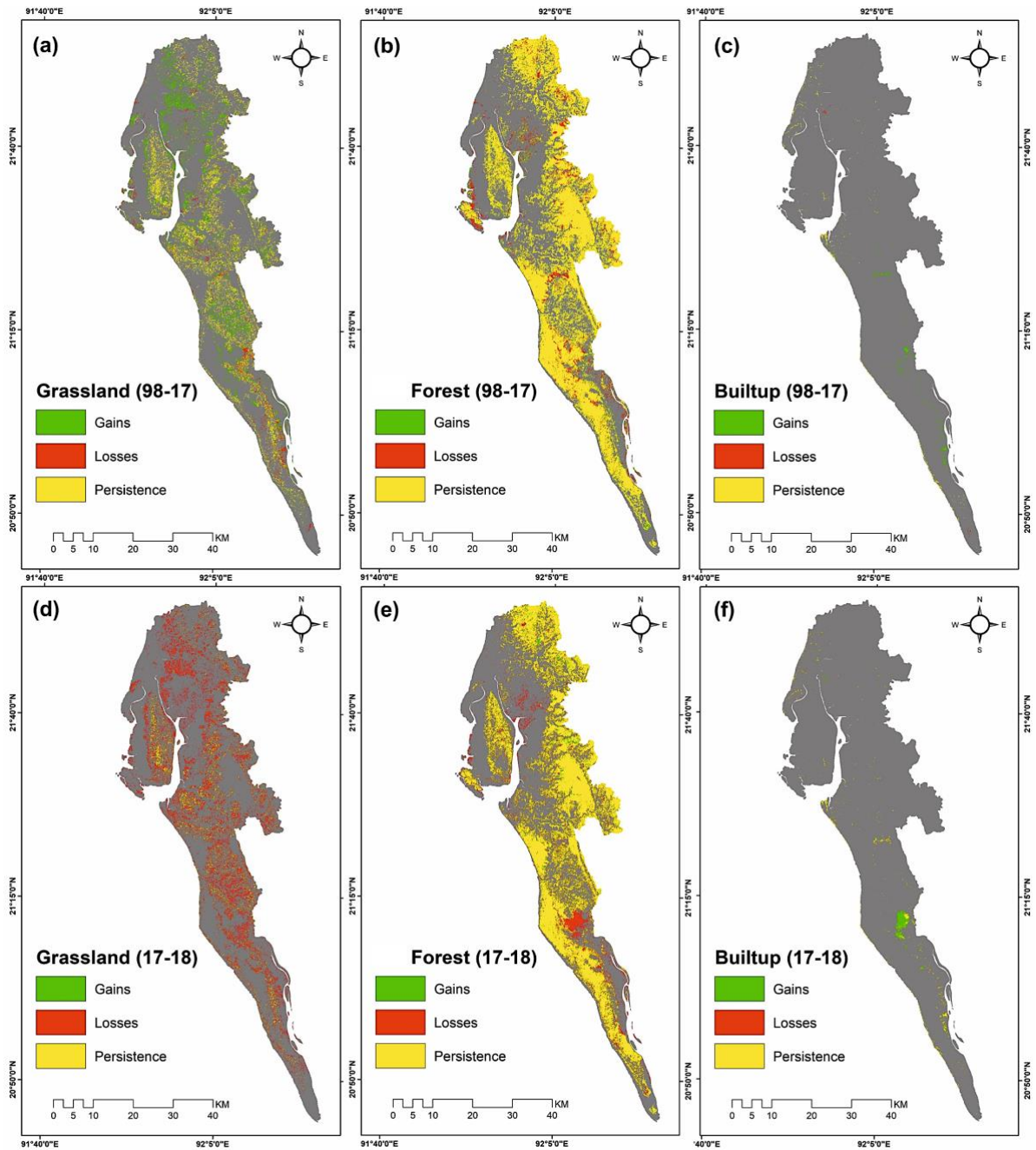
Land cover type	Area (km ²)		
	1998	2017	2018
Forest	962.73	907.62	851.87
Shrubland	0.00	33.90	221.19
Grassland	220.78	330.30	90.29
Cropland	611.25	508.37	618.61
Barren land	222.94	218.81	211.86
Waterbodies	111.83	121.00	111.71
Built-up areas	9.84	19.38	33.85

35



36 **Fig. S1.** Land cover changes between 1998-2017 and between 2017-2018 (all units
 37 are in km²).

38



39

40 **Fig. S2.** Changes in grassland, forest, and builtup areas land cover types **(a-c)**

41 between 1998–2017, **(d-f)** and between 2017–2018.

42

43

44

45

46

